Hindawi Publishing Corporation
Advances in Materials Science and Engineering
Volume 2014, Article ID 252879, 10 pages
http://dx.doi.org/10.1155/2014/252879

Review Article

New Trends in Energy Harvesting from Earth Long-Wave Infrared Emission

Luciano Mescia[1] and Alessandro Massaro[2]

[1] *Dipartimento di Ingegneria Elettrica e dell'Informazione (DEI), Politecnico di Bari, Via E. Orabona 4, 70125 Bari, Italy*
[2] *Istituto Italiano di Tecnologia (IIT), Center for Biomolecurar Nanotechnologies (CBN), Via Barsanti, 73010 Arnesano, Italy*

Correspondence should be addressed to Luciano Mescia; luciano.mescia@poliba.it

Received 12 June 2014; Accepted 18 July 2014; Published 11 August 2014

Academic Editor: Andrea Chiappini

A review, even if not exhaustive, on the current technologies able to harvest energy from Earth's thermal infrared emission is reported. In particular, we discuss the role of the rectenna system on transforming the thermal energy, provided by the Sun and reemitted from the Earth, in electricity. The operating principles, efficiency limits, system design considerations, and possible technological implementations are illustrated. Peculiar features of THz and IR antennas, such as physical properties and antenna parameters, are provided. Moreover, some design guidelines for isolated antenna, rectifying diode, and antenna coupled to rectifying diode are exploited.

1. Introduction

During the last 20 years, the worldwide energy demands have been strongly increased and as a consequence the deleterious effects of hydrocarbon-based power such as global warning, air pollution, acid precipitation, ozone depletion, and forest destruction are increasingly apparent. In order to limit these drawbacks, suitable actions aimed at reducing the dependence on the fossil fuels are needed, and the search for clean and renewable alternative energy resources is one of the most urgent challenges to the sustainable development of human civilization [1, 2].

The Sun is the most powerful source of energy providing a continuous stream of energy which warms us, causes crops to grow via photosynthesis, heats the land and sea differentially, and so causes winds and consequently waves and, of course, rain leading to hydropower. As a result, several approaches and technologies to directly or indirectly harvest energy from the Sun have been successfully proposed and implemented. In particular, in addition to the energy resources driving human society today, such as petroleum, coal, and nuclear plants, renewable energy resources, such as wind, solar, hydropower, geothermal, hydrogen, and biomass/biofuel, have been positively used to give a strong contribution to power generation without increasing environmental pollution [3].

Photovoltaic (PV) conversion is the direct conversion of sunlight into electricity without any heat engine to interfere. Photovoltaic devices are rugged and simple in design and require very little maintenance and their construction as stand-alone systems provides outputs from microwatts to megawatts. With such a vast of properties, the worldwide demand for PV is increasing every year and industry estimates suggest as much as 18 billion watts per year could ship by 2020. As a result, to meet the increased demands for solar-conversion technologies, dramatic improvements are required in terms of PV efficiency and cost/complexity reduction [4].

Solar cells convert sunlight directly into electricity. They are made of semiconducting materials that can absorb the photons from sunlight, knocking electrons from atoms to produce a flow of electricity. The energy producing aspect of the PV module has two primary steps. The first is a semiconducting material such as silicon and the second is the conversion of the electricity into direct current through an array of solar cells. The first generations of solar cells, used in 90% of today's cells, use a single p-n junction to extract energy from sunlight photons and are manufactured from silicon

semiconductors. They have about 30% efficiency but result in a price too high to compete with fossil fuels [5]. The second generations of solar cells, called thin-film solar cells, are made from amorphous silicon or nonsilicon materials and exhibit low production costs but result in much lower efficiency rates [5, 6]. The third generations of solar cells are being made from variety of new materials including solar inks, solar dyes, and conductive plastics. Some new solar cells use plastic lenses or mirrors to concentrate sunlight onto a very small piece of high efficiency PV materials [5, 7]. However, the PV material is more expensive, and because the lenses must be pointed at the Sun, the use of concentrating collectors is limited to the sunniest parts of the country.

As a quantum device, in the semiconductor solar cells only sunlight of certain energies will work efficiently to create electricity. So, the efficiency of PV is fundamentally limited by the fact that only photons with energy equal to the band gap can be efficiently harvested. For single-junction cells, the upper efficiency limit is ~30%, and with complex multijunction designs, the theoretical efficiency plateau is around 55% without excessive concentration of the incident radiation. Moreover, more complex solar cells able to harvest energy from a wider range of the electromagnetic spectrum with higher efficiency have been proposed, but they are too expensive for widespread use. However, another drawback of PV-based technologies is the fact of being strongly dependent on daylight, which in turn makes them sensitive to the weather conditions [8].

The energy created by the fusion reaction in the Sun is converted in thermal radiation and transferred in the form of electromagnetic waves into the free space. Solar radiation occurs over a wide range of wavelengths; nevertheless the main range of this radiation includes ultraviolet ($\lambda < 0.4\,\mu$m) of which the content is less than 9%, visible (light, $0.4\,\mu\text{m} < \lambda < 0.7\,\mu$m) where the content is approximately 39%, and the remaining 52% consists of infrared radiation ($0.7\,\mu\text{m} < \lambda < 100\,\mu$m). Approximately 30% of the solar radiation is scattered and reflected back to the space from the atmosphere, and about 70% is absorbed by the atmosphere and by the surface of the Earth [9]. By absorbing the incoming solar radiation, the Earth temperature rises and, as a heated object, mainly reemits electromagnetic radiation in the wavelength range from $8\,\mu$m to $14\,\mu$m with a peak wavelength of about $10\,\mu$m. Due to the different spectral properties of the Sun and Earth emission, they are classified as short-wave and long-wave infrared (LWIR) radiation, respectively. The reemitted LWIR radiation energy is underutilized by current technology.

Since the incoming LWIR is an electromagnetic wave radiation at terahertz frequencies it can be collected by tuning an antenna in such a way that it is resonant at such frequencies. This can be achieved by shrinking the dimensions of the antenna to the scale of the wavelength. To this aim, nanoantennas are an alternative approach used to scale the microwave theory down to the IR regions of the electromagnetic spectrum [10–12]. These antennas can enhance the interaction of IR waves with nanoscale matter providing a high electric field at the feeding point of the antenna [13]. In particular, this electric field generates a high-frequency alternate current or voltage which can be rectified to obtain DC current. The combination of a rectifying device at the feed points of a receiving antenna is often known as a rectenna [14–17]. Accurate numerical modeling is needed for nanoantenna performance prediction, design, and refinement as well as for obtaining some qualitative properties that may help in the design of more complex antenna array. The identification of the optimal geometric parameters and the frequency-dependent model of the permittivity of the considered materials is essential [15, 18, 19]. Moreover, the design of these novel antennas by using well-known printing techniques allowing costs reduction and a quick prototyping approach is another important aspect to consider. To this aim, in this paper an overview of the rectenna system is provided, detailing principles of operation, antenna designs, materials, and fabrication. Moreover, some recent technologies pertaining to both the nanoantennas and the rectifying diodes fabrication are also presented. In particular, the physical properties of nanoantennas, the nanoantenna parameters, and the computational considerations as well as important aspects pertaining to the radiation efficiency, directivity, bandwidth, polarization, and impedance matching are illustrated.

2. The Rectenna Topology

Although nanoantennas capture infrared energy they need a rectifier to recover energy; these devices which couple rectifiers to nanoantennas are also known as rectennas. The rectenna is a special type of antenna used to directly convert microwave energy into DC electricity. The idea of collecting solar electromagnetic radiation with a rectenna was proposed three decades ago [20] but it has not yet been fully achieved. However, this technology has been fruitfully used in microwave energy harvesting for space solar power satellite applications [21, 22], wireless power transmission [23], low power electronics [24–26], and hybrid harvesters [27, 28].

In the rectenna system, the absorption of the incident electromagnetic radiation occurs at the resonant frequency of the antenna. In particular, when the resonant mode is excited, a cyclic plasma movement of free electrons is induced in the metal antenna. The electrons freely flow along the antenna, generating alternating current at the same frequency as the resonance flowing toward the antenna feed point. However, antennas do not provide a means of converting the collected power at high frequencies into DC power; so this will need to be accomplished by a transducer, such as rectifier. A typical rectenna block diagram is present in Figure 1. It consists of a nanoantenna, a low-pass filter (LPF), a rectifying circuit, a LPF for DC path, and a load. The nanoantenna collects the IR incoming power; the input low-pass filter provides matching between the antenna and the rectifier as well as suppressing the unwanted higher harmonics rejected by the rectifying circuit. The rectifying circuit, typically a diode, rectifies the AC current induced in the antenna, and the DC pass filter provides a DC path to the load by separating the high-frequency components from the DC signal [23].

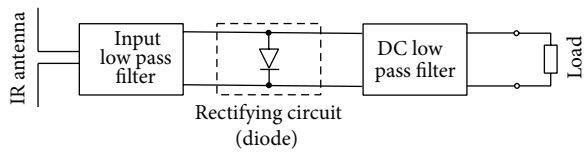

Figure 1: Block diagram of rectenna.

2.1. Isolated IR Antenna. In recent years, the use of nanoantennas has gained a great interest for solar energy harvesting [10, 15, 18, 29]. These antennas couple electromagnetic radiation at very high frequencies, THz, and IR regimes in the same way that RF antennas do at the corresponding wavelengths. As a consequence, several studies are currently focused on translating the concepts of RF antennas into the optical frequency regime.

Because the size of nanoantennas is in the range from a few hundred nanometres to a few microns, the technological limits did not allow their realization until a few years ago. However, thanks to the development of electron-beam lithography and similar techniques the required level of miniaturization for the realization and demonstration of nanoantennas has been obtained [13, 30, 31]. Nanoantennas exhibit potential advantages in terms of polarization, tunability, and rapid time response [10, 29]. In fact, they have (i) a very small detection area, they (ii) allow the electromagnetic field localization beyond the diffraction limit, (iii) they very efficiently release radiation from localized sources into the far field, (iv) they make possible the tailoring of the interaction of electromagnetic field at the nanoscale, and (v) they can be tuned to a specific wavelength. Finally, the nanoscale antenna dimensions combined with the high electric field enhancement in the antenna gap enable a small device footprint making it compact enough to be monolithically integrated with electronics and auxiliary optics.

The guidelines for the nanoantenna design are quite similar to those used at RF frequencies, but crucial differences in their physical properties and scaling behavior occur. In fact, in contrast to perfectly conducting concept used at RF frequencies, at optical frequencies metals no longer behave as perfect conductors and their interaction with electromagnetic field is determined by the frequency-dependent complex dielectric function [32]. In particular, the Lorentz-Drude model is generally used to explain the dispersive behavior of the metal [33, 34]:

$$\varepsilon_r(\omega) = \varepsilon_r^f(\omega) + \varepsilon_r^b(\omega), \tag{1}$$

where $\varepsilon_r^f(\omega)$ describes the free-electron effects (intraband) and $\varepsilon_r^b(\omega)$ describes the bound-electron effects (interband). In particular, the intraband contribution is described by the Drude model:

$$\varepsilon_r^f(\omega) = 1 - \frac{\Omega_p^2}{\omega(\omega - i\Gamma_0)}, \tag{2}$$

while the interband contribution is described by the model resembling the Lorentz result for insulators:

$$\varepsilon_r^b(\omega) = \sum_{j=1}^{k} \frac{f_j \omega_p^2}{\left(\omega_j^2 - \omega^2\right) + i\omega\Gamma_j}, \tag{3}$$

where ω_p is the plasma frequency, k is the number of oscillators with frequency ω_j, strength f_j, and lifetime $1/\Gamma_j$, and Ω_p is the plasma frequency of the intraband transitions with oscillator strength f_0 and damping constant Γ_0. The availability of this model also allows the calculation of the skin depth which at optical frequencies is comparable with the dimensions of the antenna. As a result, the resonant length of the antenna does not exactly scale linearly with the incident frequency; thus in order to better evaluate the antenna parameters, an effective wavelength λ_{eff} should be calculated [10, 35]:

$$\lambda_{\text{eff}} = n_1 + n_2 \frac{\lambda}{\lambda_p}, \tag{4}$$

where λ_p is the plasma wavelength of the metal and n_1 and n_2 are constant values depending on the geometry and dielectric parameters of the antenna.

The radiation efficiency, directivity, and bandwidth of the antenna are critical parameters to take into account. To this aim, to assess the overall antenna efficiency a figure of merit FoM is often defined in terms of half-power beam width, fractional bandwidth, and peak gain [12, 36]. Moreover, the design of the best antenna for a given application is a problem not easy to solve because of contradicting requirements. In fact, a strong directivity, a large bandwidth, a small size, and a large radiation resistance need to be combined. Furthermore, the typical design strategies of the radio wave antenna engineering cannot be completely used without careful considerations. In fact, at the THz and IR frequencies the metal losses became a constraint that antenna and circuit engineering have to take into account. Rather a lot of the energy in the surface modes is carried in the dielectric above the antenna. Compared to RF regime, the large losses and the finite skin depth generate consequences as reduced radiation efficiency, lower quality factor of the resonances, deviating radiation patterns, and current distribution. Finally, the well-known impedance matching circuits based on passive stub-like resonator structures have to be carefully designed since the metal losses strongly reduce the overall radiation efficiency [10, 32].

One important aspect that a rectenna has to verify is that it should be able to concentrate the propagating free-space LWIR plane waves having a wide spectral bandwidth and incoming from a range of directions of incidence. As a result, the design of the isolated antenna plays an important role for the overall rectenna efficiency. Among various types of antenna, planar antennas are gaining popularity owing to their low profile, light weight, and simple coupling with rectifying element [12, 16, 17]. In addition, they offer versatility in terms of resonant frequency, polarization, radiation pattern, and impedance. They are supported by a substrate and considering that it is electrically thicker, at THz

frequencies a decreased efficiency occurs with respect to their RF counterparts. In order to overcome this drawback, printed antennas having grounded substrates are generally preferred. In fact, due to the image dipole generated by the ground interface the antenna impedance is modified and substrate thickness can be reduced to increase the efficiency. Moreover, the presence of the ground allows the radiation in only one direction. On the contrary, the radiation properties of these antennas become sensitive to substrate losses, especially when the substrate thickness increases, and the substrate permittivity acting as a parasitic impedance causes a red shift of the resonant frequency. As a result, for a given substrate permittivity there is a particular substrate thickness maximizing the performance of the printed antennas. Until now, dipole [11, 14, 15, 37], crossed dipole [12, 38], bowtie [11, 39, 40], log-periodic [11, 41], square-spiral [13, 18], and Archimedean spiral [11, 42] geometries have been proposed for IR and THz antennas.

Half-wave dipoles could be designed to have purely real input impedance; thus no conjugate impedance match occurs. Their very good directivity is attractive in terms of enhanced sensitivity for detection. The input impedance, current distribution, radiation efficiency, broadside gain, effective area, and effective length depend on the arm size, frequency, and employed metal [11, 14]. In particular, the physical length is shorter but close to half the wavelength and decreases by increasing the arm thickness. Moreover, the interelement distance affects input impedance and field enhancement in the feed-gap region [37]. Unfortunately, this kind of antenna does not allow flexibility to increase or optimize the electric field in the gap. The only approach is to vary the gap size or increase the rods width.

The bowtie antenna could be a good candidate to replace the dipole antenna. It is constituted of two triangles facing each other tip to tip. This configuration allows a simple design and broadband impedance and makes possible the modification of several antenna parameters. In fact, gap size, apex angle, and antenna dimensions could be tuning to increase the captured electric field in the gap. Moreover, because they represent the two-dimensional analogue of a biconical antenna they possess a broad bandwidth. Another advantage of bowtie antennas is the ability of building an array by coupling many elements and combining the electric field from each element at array feeding point, where a rectifier can be embedded. In order to consider bowtie antennas for practical applications a finite gap between the feed points and a finite size have to be used. Generally, these constraints result in limited bandwidth but no significant effect on the radiation pattern or the impedance typically occurs if the antenna is terminated with a bow-arm length of $2\lambda_{\text{eff}}$ [11].

Due to their broad bandwidth, spiral antennas have been proposed to collect solar energy [13, 18]. They allow concentrating the electric field in the gap between two metallic arms which constitutes an appropriate point to transport energy needed to supply other circuitries. These antennas are good resonators and it is expected to capture a large electric field at resonance. Moreover, the gain performance of the spiral antenna can be easily improved by increasing the number of arms. Round spiral antennas are generally designed by using Archimedean spiral geometries which have linear growth rates and frequency independent radiative characteristics. Moreover, the frequency independency is limited to a wavelength band determined by the antenna size. Spiral antennas can be constructed as planar structures and they can radiate linearly or circularly polarized waves. The optimal reception of a spiral antenna occurs when the spiral arm length equals approximately one wavelength, which corresponds to a diameter of $D = \lambda_{\text{eff}}/\pi$, for the circular spiral, and a side length $W = \lambda_{\text{eff}}/4$ for the square spiral. According to these relations, square-spiral geometries have more advantages in terms of size with respect to circular ones because comparable antenna gain can be obtained when the width of the square spiral is approximately 75% of the diameter of the circular spiral antenna. However, the main drawback with this type of antenna is the difficulty in configuring an array. Despite that, equiangular spiral can be chosen as the array element since it allows (i) convenient connection of DC lines at the tips of the spiral arms, (ii) possible dual polarization, and (iii) convenient feed point for diode connection.

Although the THz and IR antennas are usually synthesized by means of basic and somewhat simple elements, the lack of guidelines for the synthesis process as well as the absence of mature theory and design equations for nanoantennas makes the computational tools very useful to fulfill complex or nonstandard design requirements. In fact, considering that the antenna design usually involves the optimization of a multidimensional parameter space a careful investigation of proper global optimization tools has to be performed in order to reduce the severe computational limits due to the expensive discretizations due to the numerical modeling. To this aim, efficient optimization tools based on stochastic optimization techniques such as genetic algorithms and particle swarm optimization have been efficiently employed in the antenna synthesis [43].

2.2. IR Antenna Coupled to Rectifying Diode. As mentioned above, a suitable choice of the antenna material as well as an accurate design of the antenna has to be fulfilled to improve the coupling efficiency of the free-space radiation into the antenna. However, a suitable rectifier has to be attached to the antenna to obtain a DC signal. As a consequence, the RF-to-DC conversion efficiency of a rectenna is influenced by the amount of power loss in the diodes, by the impedance match between the antenna and the rectifier and between the rectifier and the load, and also by the antenna efficiency. In fact, nonoptimized element design, impedance mismatch between components, and inefficient rectifying junctions could contribute to unsuccessful collection of the incoming electromagnetic energy.

Figure 2 shows the equivalent circuit of the antenna coupled to rectifying diode. The receiving antenna, when operating at its resonant frequency, can be modeled by a voltage source, V_{open}, and an impedance in series, $Z_A = R_A + jX_A$. In particular, V_{open} is the open circuit voltage occurring at the end of the antenna when no load is connected and Z_A

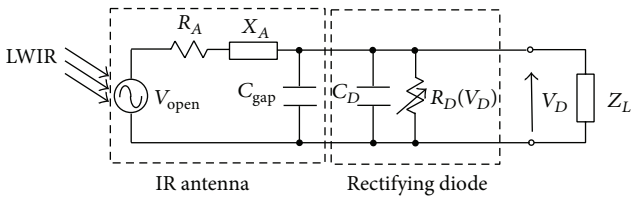

Figure 2: Circuit model of IR antenna coupled to rectifying diode.

is the antenna impedance, where X_A is the antenna reactance and R_A is the antenna resistance which is a combination of the radiation resistance, modelling the radiated power, in series with the loss resistance and modelling the conductive and dielectric losses. Moreover, the capacitance, C_{gap}, generated by the air gap should be considered in order to rightly model two-arm antenna.

The rectifying diode is generally characterized by a threshold voltage, a junction capacitance, C_D, and a nonlinear series resistance, R_D. The junction capacitance has an impact on diode switching time; a fast diode should have small junction capacitance. In fact, the cutoff frequency f_c, characterizing the frequency response of the diode, effectively depends on both the diode resistance and capacitance as follows:

$$f_c = \frac{1}{2\pi R_D C_D}. \tag{5}$$

So, considering that the resistance R_D mainly depends on the fabrication process, the cutoff frequency can be tuned by adjusting the capacitance C_D. However, the presence of the antenna resistance modifies the overall device response so that the cutoff frequency of the device is evaluated by the following relation:

$$f_c = \frac{R_A + R_D}{2\pi R_A R_D \left(C_{gap} + C_D\right)}. \tag{6}$$

Moreover, the threshold voltage is a very important factor to consider, especially when low power levels have to be harvested. So, for rectification purpose a low-cutoff voltage diode has to be selected.

The voltage V_{open} can be expressed as

$$V_{open} = 2E_i \sqrt{\frac{R_A A_{eff}}{Z_0}}, \tag{7}$$

where E_i is the incident electric field, A_{eff} is the effective area of the antenna, and Z_0 is the intrinsic impedance of free space. Moreover, A_{eff} is defined as

$$A_{eff} = \frac{\lambda^2 G}{4\pi}, \tag{8}$$

where G is the antenna gain and λ is the free-space wavelength. The amplitude of the incident electric field can be calculated as

$$E_i = \sqrt{2Z_0 P_i}, \tag{9}$$

where P_i is the incident power density. In particular, considering the thermal radiation emitted by the Earth, the incident power can be expressed in terms of the radiation emitted by a black body at the temperature T per unit of area and wavelength [44]

$$P_i(\lambda, T) = \frac{2\pi c^2 h}{\lambda^5} \frac{1}{\exp\left(hc/\lambda\kappa T\right) - 1}, \tag{10}$$

where c is the speed of light, T is the temperature expressed in Kelvin degree, $P_i(\lambda, T)d\lambda$ is the amount of the power emitted in the wavelength range from λ to $\lambda + d\lambda$ per unit of area, unit of time, and unit of solid angle, and h and κ are the Plank and Boltzmann constant, respectively. Using (7)–(9) the final expression of the open circuit voltage is

$$V_{open} = \sqrt{\frac{2R_A\lambda^2 G}{\pi} P_i}. \tag{11}$$

Considering the equivalent circuit illustrated in Figure 2 the power delivered to the load Z_L is given by the following equation:

$$P_L = \frac{1}{2} \frac{R_D}{\left(R_A + R_D\right)^2 + \left(X_A + X_D\right)^2} \left|V_{open}\right|^2 \tag{12}$$

or using (11)

$$P_L(\lambda, T) = \frac{1}{\pi} \frac{R_A R_D \lambda^2 G}{\left(R_A + R_D\right)^2 + \left(X_A + X_D\right)^2} P_i(\lambda, T). \tag{13}$$

Considering the frequency dependence of the incident power density, the total received power over a range of frequencies is given by

$$P_{L,tot} = \int_{\lambda_1}^{\lambda_2} P_L d\lambda = \int_{\lambda_1}^{\lambda_2} \frac{1}{\pi} \frac{R_A R_D \lambda^2 G P_i}{\left(R_A + R_D\right)^2 + \left(X_A + X_D\right)^2} d\lambda, \tag{14}$$

where λ_1 and λ_2 are the starting and stopping wavelengths.

The RF-to-DC conversion efficiency of the rectenna is usually defined as the ratio between the power delivered to the load (harvest DC power) and the amount of the power that the receiving antenna could inject in a perfectly matched circuit:

$$\eta = \frac{P_{DC}}{P_{i,tot}} = \frac{P_{DC}}{\int_{\lambda_1}^{\lambda_1} A_{eff} P_i d\lambda}. \tag{15}$$

The nonlinear nature of diodes complicates the analytical evaluation of the conversion efficiency. In fact, for most rectifier circuits the P_{DC} depend on input power $P_{L,tot}$, operating frequency, impedance matching, and diode properties. In particular, a good model to estimate η is

$$\eta = \frac{V_D I_{out}}{\left(1/T_{RF}\right) \int_0^{T_{RF}} v_{in}(t)\, I_{DC}(t)\, dt}, \tag{16}$$

where T_{RF} is the period of the input RF signal, v_{in} is the input voltage to the rectifier, I_{out} is the current flowing through the load terminals, $I_{DC}(t)$ is the current flowing through the diode terminals, and V_D is the DC voltage.

This circuit model illustrated in Figure 2 gives quite detailed information on how the THz and IR solar rectenna works, including the parameters affecting its performance. However, the main limitation of this circuit is that a good RF-to-DC conversion efficiency is given for a well-defined operation point characterized by a specific input power level, central frequency, and load impedance. Outside these operating parameters the energy conversion efficiency strongly decreases. In fact, rectenna structure well works for an optimal input power level and becomes inefficient at another power level. This problem is very huge since harvesting systems generally are required to operate at variable workload conditions to dynamically track voltage levels while conserving energy. In order to overcome these limitations, specific design procedures have to be fulfilled in terms of load and power matching. Typical solutions are based on the use of maximum power point tracking voltage boost stage [45], a dynamic switching conversion scheme based on active control for harvesting energy [46], and modified Greinacher rectifier [47].

2.3. Rectifying Element. There are a number of issues related to the development of a rectenna. Firstly, the antenna elements need to be extremely small. Another difficulty is making diodes with small physical size, small turn-on voltage, and efficient operation at THz and IR frequencies able to rectify the received signals to DC as a usable output. Moreover, to efficiently convert electromagnetic energy and to take full advantage of the enhanced electric field in the center gap of the antenna, the diode should be coplanar and coupled to the antenna. As a result, the development of diode technology is the key challenge to demonstrate the feasibility of rectenna to convert the thermal Earth radiation in DC current.

Low power Schottky diodes are used for rectification and detection in the low frequency regime up to 5 THz [48]. In fact, due to their ultrafast transport mechanism they are scalable to very high frequencies by reducing their physical contact area. The most important advantages of the Schottky diode are the lower forward resistance and lower noise generation. However, the fabrication of large arrays requires challenging efforts and additional engineering issues are needed for their coupling with antennas.

A promising alternative is the unipolar nanodiodes known as self-switching devices (SSDs) [49, 50]. These devices are based on an asymmetric nanochannel which results in a nonlinear, diode-like, current-voltage characteristic but without using any doped junctions or any tunneling barriers. Their threshold voltage only depends on the geometry and zero-threshold detectors can be easily fabricated. Moreover, a single fabrication step needs for the fabrication of arrays a large number of SSDs connected in parallel. The SSD has been demonstrated in a variety of materials, including two-dimensional electron gases (2DEGs) in GaAs [50] and InGaAs [51], silicon on insulator [52], and both organic [53] and metal-oxide [54] thin films.

Antenna-coupled microbolometer detectors have been demonstrated in the infrared at wavelengths near 10 μm. The operation principle of these devices is based on change of the bolometer resistance with an increase in the temperature. In particular, their advantages are the room temperature operation as well as their tunability for wavelength and polarization response [31, 55, 56].

The diodes can be classified in low voltage tunnel type diodes and ultralow-voltage diodes. Examples of low voltage tunnel diodes are studied in [57], where different tunneling junction dimensionalities exhibit different turn-on characteristics. The most popular rectifier in THz and IR rectennas is the metal-insulator-metal (MIM) diode. It is a thin-film device in which the electrons tunnel through the insulator layer from the first metal layer to the second metal [15]. The main advantages of these diodes are small size, CMOS compatibility, and ability to offer full functionality without cooling and applied bias. The rectification is based on the electron tunneling process occurring through the insulator layer. The study of inorganic (the insulator used can be the nickel oxide) and organic (the insulator used can be polyaniline, thiol) MIM tunnel junctions has been discussed in [58]. This study was oriented on solar/thermal energy conversion efficiency by converting waste heat to electrical energy using rectenna discussing the implementation of self-assembled monolayers (SAMs) as alkanethiol SAMs. For a successful rectification, the I-V characteristics of a MIM diode should be nonlinear and asymmetrical with no external bias applied. Moreover, the insulator layer should be very thin to allow sufficiently large electrical current and to ensure the occurrence of the tunneling effect. To this aim, MIM diodes fabricated with dissimilar metals on both sides of the insulator layer result in higher efficiency energy conversion than with similar metals. When operating in higher frequencies, greater optimization of the device is required to address low impedance and high nonlinearity. Moreover, in order to allow the rectification at THz frequencies the diode area has to be very small.

Ultralow-voltage diodes are ballistic with geometrical asymmetry and are characterized by a low capacitance. Two-dimensional ballistic nanodevices could be able to rectify an electric signal if the device has a taper-type nonuniform cross section [59]. Tapered profiles can be also considered in Au/SiO_2 or Au/Si plasmon waveguide for nanoscale focusing of light at 830 nm [60] and also for midinfrared energy [61]. Considering innovative materials, graphene could be implemented for rectennas improving performances oriented on THz resonator material and rectifying 10.6 μm radiation corresponding to an operating frequency of 28 THz [62]. The ballistic rectifier can be also manufactured by means of GaAs-AlGaAs heterostructures in asymmetric microjunction configuration [63].

2.4. Technological Aspects and Materials. As discussed in previous sections, significant progress in improving the overall

rectenna efficiency can be obtained through a careful design to efficiently match the broadband, arbitrarily polarized nature of the radiation energy reemitted by the Earth. In addition, the introduction of innovative layouts and materials could provide a broadband, high conversion efficiency low-cost solution supporting conventional photovoltaic solar cells. Moreover, a little added cost by integrating the plasmonic emitter with the cell could significantly increase the efficiency of photovoltaic PV cells [64]. In this direction, CP1 polymer material can be used for both IR transmissive and electrically conductive materials for MEMS based thermal device in satellites [65]; other polyimides tend to be expensive, absorb too much solar energy, have lower UV resistance, and are not as transparent as CP1, degrading more rapidly in the space environment. Planar metal-insulator-metal (MIM) diodes cannot provide a sufficiently low RC time constant to rectify visible light but could be easily integrated in solar rectennas [66]. Thermal infrared light represents an extreme challenge to harvest efficiently using planar MIM diodes: their large RC time orients the diodes on visible light frequency rectification; they can work at low terahertz frequencies, but for thermal infrared frequencies of ~30 THz and higher they cannot respond efficiently. Radiative cooling devices should ideally work with a substrate blocking solar radiation but it is transparent around 8–13 μm. An innovative new type of material for radiative cooling applications is the polyethylene foils pigmented with nanocrystalline TiO_2 [67] providing high IR transmittance and high solar reflectance. Titania nanoparticles are also suitable for high-resonant energy photons allowing a broad solar spectral absorption [68] from the visible and near-infrared domain. Considering nanocomposite materials, which are made by a polymer with the introduction of nanofillers improving optical and physical properties [69], NIR reflectance efficiency for solar thermal control interface films was found for PMMA/ZnO nanoparticles [70]. Also dye-sensitized solar cells could utilize nanomaterials, such as semiconductor nanowires, nanocones, nanotubes, and nanofibers, which could be prepared by chemical vapour deposition (CVD), colloidal lithography, template-guided deposition, or electrospinning technique [71]. Optoelectronic emissive energy harvester is commonly implemented by rectenna. In particular, concerning technology, the antennas could be fabricated by high-resolution electron-beam lithography and metal lift-off on double-side-polished silicon substrates using polymethyl methacrylate as electron-sensitive polymer and by thermally evaporated gold [61].

The fabrication of THz and IR antenna requires reliable and reproducible structuring techniques able to accurately define critical antenna dimensions such as gap size and arm length. Various top-down and bottom-up nanofabrication approaches have been applied to experimentally realize these kinds of antennas. In particular, top-down approaches such as electron-beam lithography (EBL) [72, 73] and focused-ion beam (FIB) milling [74] are capable of fabricating large arrays of nearly identical nanostructures with defined orientation and distances. On the other hand, bottom-up approaches take advantage of chemical synthesis and self-assembly of nanoparticles in solution but they often require precise size selection and nanopositioning as well as assembly strategies to create nontrivial structures.

EBL could be a convenient way to systematically investigate dimensions, spacing, and geometrical effects in a controlled manner. Recently, electron-beam induced deposition has been applied to build complex nanostructures [72]. Moreover, this technique could be applied to engineering of the dielectric properties of the antenna environment. Considering the high versatility of the direct patterning approach, the FIB milling has been successfully applied in a realization of a number of optical antennas. Therefore, this technique ensures a very good resolution and can be adopted to almost any type of material. However, considering that both EBL and FIB are very slow and expensive they do not support large-scale manufacturing. Possible alternatives are nanoimprint lithography (NIL) [75] and roll-to-roll (R2R) processing [76]. The particular advantage of NIL compared to other lithography techniques is the ability to fabricate large-area and complex 3D micro/nanostructures with low-cost and high throughput. The most important variety of NIL process types demonstrating a sub-10 nm resolution is the hot embossing lithography (HEL) or thermal nanoimprint lithography (TNIL) and the UV-based nanoimprint lithography (UV-NIL). However, in recent years a variety of new processes have been proposed and investigated, such as reverse NIL, soft UV-NIL, laser assisted direct imprint (LADI), sub-10 nm NIL, chemical nanoimprint, and electrical field-assisted NIL [77]. For conventional NIL processes, the most important problem is that it cannot significantly improve the throughput in the patterning of large-area product with low cost because it is not a continuous process. To overcome this limitation, roller-type nanoimprint lithography (RNIL) [78, 79] has been developed, and due to the continuous process, simple system construction, high throughput, low cost, and low energy consuming this technology is becoming the most potential manufacturing method for industrialization of nanoimprinting process. However, in future, NIL might become the ideal technique for low-cost, highly reproducible realization of antenna arrays covering large areas.

3. Conclusion

The progress and the challenges of rectenna to harvest energy from Earth long-wave infrared emission have been reviewed. The rectenna system can be made from different conducting metals and dielectric materials, a variety of broadband antennas, and a number of rectifying devices. The use of broadband antennas for collection of long-wave infrared Earth's energy has a big potential advantage. As a result, the accurate design of the antenna is a key topic to improve the electricity generation efficiency of the overall system. The study of IR and THz antennas is still in its initial stage and extensive research needs to be performed to improve the matching efficiency due to the mismatch between antenna and rectifier impedance as well as to produce maximum electric field enhancement at the feeding point of the antenna. Moreover, further research activities have to be fulfilled to identify the suitable materials and technology for the design and fabrication of efficient THz rectifiers.

Conflict of Interests

The authors declare that there is no conflict of interests regarding the publication of this paper.

References

[1] F. Manzano-Agugliaro, A. Alcayde, F. G. Montoya, A. Zapata-Sierra, and C. Gil, "Scientific production of renewable energies worldwide: an overview," *Renewable and Sustainable Energy Reviews*, vol. 18, pp. 134–143, 2013.

[2] A. Arigliano, P. Caricato, A. Grieco, and E. Guerriero, "Producing, storing, using and selling renewable energy: the best mix for the small medium industry," *Computers in Industry*, vol. 65, no. 3, pp. 408–418, 2014.

[3] A. Khaligh and O. G. Onar, *Energy Harvesting: Solar, Wind, and Ocean Energy Conversion Systems*, CRC Press, 2010.

[4] G. N. Tiwari and S. Dubey, *Fundamentals of Photovoltaic Modules and Their Applications*, RSC Publishing, 2010.

[5] V. V. Tyagi, N. A. A. Rahim, and J. A. L. Selvaraj, "Progress in solar PV technology: research and achievement," *Renewable and Sustainable Energy Reviews*, vol. 20, pp. 443–461, 2013.

[6] C. Becker, D. Amkreutz, T. Sontheimer et al., "Polycrystalline silicon thin-film solar cells: status and perspectives," *Solar Energy Materials and Solar Cells*, vol. 119, pp. 112–123, 2013.

[7] Z. Abdin, M. A. Alim, R. Saidur et al., "Solar energy harvesting with the application of nanotechnology," *Renewable and Sustainable Energy Reviews*, vol. 26, pp. 837–852, 2013.

[8] A. Goetzberger and V. U. Hoffmann, *Photovoltaic Solar Energy Generation*, Springer, Berlin, Germany, 2005.

[9] G. L. Stephens, J. Li, M. Wild et al., "An update on Earth's energy balance in light of the latest global observations," *Nature Geoscience*, vol. 5, no. 10, pp. 691–696, 2012.

[10] P. Bharadwaj, B. Deutsch, and L. Novotny, "Optical Antennas," *Advances in Optics and Photonics*, vol. 1, no. 3, pp. 438–483, 2009.

[11] F. J. González and G. D. Boreman, "Comparison of dipole, bowtie, spiral and log-periodic IR antennas," *Infrared Physics & Technology*, vol. 46, no. 5, pp. 418–428, 2005.

[12] I. Kocakarin and K. Yegin, "Glass superstrate nanoantennas for infrared energy harvesting applications," *International Journal of Antennas and Propagation*, vol. 2013, Article ID 245960, 7 pages, 2013.

[13] D. K. Kotter, S. D. Novack, W. D. Slafer, and P. J. Pinhero, "Theory and manufacturing processes of solar nanoantenna electromagnetic collectors," *Journal of Solar Energy Engineering*, vol. 132, no. 1, Article ID 011014, 9 pages, 2010.

[14] Z. Ma and G. A. E. Vandenbosch, "Optimal solar energy harvesting efficiency of nano-rectenna systems," *Solar Energy*, vol. 88, pp. 163–174, 2013.

[15] A. M. A. Sabaawi, C. C. Tsimenidis, and B. S. Sharif, "Analysis and modeling of infrared solar rectennas," *IEEE Journal on Selected Topics in Quantum Electronics*, vol. 19, no. 3, Article ID 9000208, 2013.

[16] S. Shrestha, S. Noh, and D. Choi, "Comparative study of antenna designs for RF energy harvesting," *International Journal of Antennas and Propagation*, vol. 2013, Article ID 385260, 10 pages, 2013.

[17] S. Shrestha, S. R. Lee, and D.-Y. Choi, "A new fractal-based miniaturized sual band patch antenna for RF energy harvesting," *International Journal of Antennas and Propagation*, vol. 2014, Article ID 805052, 9 pages, 2014.

[18] M. Gallo, L. Mescia, O. Losito, M. Bozzetti, and F. Prudenzano, "Design of optical antenna for solar energy collection," *Energy*, vol. 39, no. 1, pp. 27–32, 2012.

[19] M. Bozzetti, G. De Candia, M. Gallo, O. Losito, L. Mescia, and F. Prudenzano, "Analysis and design of a solar rectenna," in *Proceeding of the IEEE International Symposium on Industrial Electronics (ISIE '10)*, pp. 2001–2004, Bari, Italy, July 2010.

[20] R. L. Bailey, "Proposed ne w concept for a solar-energy converter," *Journal of Engineering for Gas Turbines and Power*, vol. 94, no. 2, pp. 73–77, 1972.

[21] R. Wang, D. Ye, S. Dong et al., "Optimal matched rectifying surface for space solar power satellite applications," *IEEE Transactions on Microwave Theory and Techniques*, vol. 62, pp. 1080–1089, 2014.

[22] A. Takacs, H. Aubert, S. Fredon, L. Despoisse, and H. Blondeaux, "Microwave power harvesting for satellite health monitoring," *IEEE Transactions on Microwave Theory and Techniques*, vol. 62, pp. 1090–1098, 2014.

[23] Z. Ma and G. A. E. Vandenbosch, "Wideband harmonic rejection filtenna for wireless power transfer," *IEEE Transactions on Antennas and Propagation*, vol. 62, no. 1, pp. 371–377, 2014.

[24] U. Alvarado, A. Juanicorena, I. Adin, B. Sedano, I. Gutiérrez, and J. De Nó, "Energy harvesting technologies for low-power electronics," *European Transactions on Telecommunications*, vol. 23, no. 8, pp. 728–741, 2012.

[25] K. W. Lui, A. Vilches, and C. Toumazou, "Ultra-efficient microwave harvesting system for battery-less micropower microcontroller platform," *IET Microwaves, Antennas and Propagation*, vol. 5, no. 7, pp. 811–817, 2011.

[26] J. Masuch, M. Delgado-Restituto, D. Milosevic, and P. Baltus, "Co-integration of an RF energy harvester into a 2.4 GHz transceiver," *IEEE Journal of Solid-State Circuits*, vol. 48, no. 7, pp. 1565–1574, 2013.

[27] A. Collado and A. Georgiadis, "Conformal hybrid solar and electromagnetic (EM) energy harvesting rectenna," *IEEE Transactions on Circuits and Systems I: Regular Papers*, vol. 60, no. 8, pp. 2225–2234, 2013.

[28] T. Peter, T. A. Rahman, S. W. Cheung, R. Nilavalan, H. F. Abutarboush, and A. Vilches, "A novel transparent UWB antenna for photovoltaic solar panel integration and RF energy harvesting," *IEEE Transactions on Antennas and Propagation*, vol. 62, pp. 1844–1853, 2014.

[29] J. Alda, J. M. Rico-García, J. M. López-Alonso, and G. Boreman, "Optical antennas for nano-photonic applications," *Nanotechnology*, vol. 16, no. 5, pp. S230–S234, 2005.

[30] M. Bareiss, B. N. Tiwari, A. Hochmeister et al., "Nano antenna array for terahertz detection," *IEEE Transactions on Microwave Theory and Techniques*, vol. 59, no. 10, pp. 2751–2757, 2011.

[31] M. A. Gritz, I. Puscasu, D. Spencer, and G. D. Boreman, "Fabrication of an infrared antenna-coupled microbolometer linear array using chrome as a mask," *Journal of Vacuum Science and Technology B*, vol. 21, no. 6, pp. 2608–2611, 2003.

[32] P. Biagioni, J.-S. Huang, and B. Hecht, "Nanoantennas for visible and infrared radiation," *Reports on Progress in Physics*, vol. 75, no. 2, Article ID 024402, 2012.

[33] A. D. Rakić, A. B. Djurišić, J. M. Elazar, and M. L. Majewski, "Optical properties of metallic films for vertical-cavity optoelectronic devices," *Applied Optics*, vol. 37, no. 22, pp. 5271–5283, 1998.

[34] R. Qiang, R. L. Chen, and J. Chen, "Modeling electrical properties of gold films at infrared frequency using FDTD

method," *International Journal of Infrared and Millimeter Waves*, vol. 25, no. 8, pp. 1263–1270, 2004.

[35] L. Novotny, "Effective wavelength scaling for optical antennas," *Physical Review Letters*, vol. 98, Article ID 266802, 2007.

[36] S. Ladan, N. Ghassemi, A. Ghiotto, and K. Wu, "Highly efficient compact rectenna for wireless energy harvesting application," *IEEE Microwave Magazine*, vol. 14, no. 1, pp. 117–122, 2013.

[37] A. Locatelli, "Analysis of the optical properties of wire antennas with displaced terminals," *Optics Express*, vol. 18, no. 9, pp. 9504–9510, 2010.

[38] J. L. Stokes, Y. Yu, Z. H. Yuan et al., "Analysis and design of a cross dipole nanoantenna for fluorescence-sensing applications," *Journal of the Optical Society of America B*, vol. 31, pp. 302–310, 2014.

[39] E. Briones, J. Alda, and F. J. González, "Conversion efficiency of broad-band rectennas for solar energy harvesting applications," *Optics Express*, vol. 21, no. 3, pp. A412–A418, 2013.

[40] P. M. Krenz, B. Tiwari, G. P. Szakmany et al., "Response increase of IR antenna-coupled thermocouple using impedance matching," *IEEE Journal of Quantum Electronics*, vol. 48, no. 5, pp. 659–664, 2012.

[41] A. D. Semenov, H. Richter, H. W. Hübers et al., "Terahertz performance of integrated lens antennas with a hot-electron bolometer," *IEEE Transactions on Microwave Theory and Techniques*, vol. 55, pp. 239–247, 2007.

[42] S. Cherednichenko, A. Hammar, S. Bevilacqua, V. Drakinskiy, J. Stake, and A. Kalabukhov, "A room temperature bolometer for terahertz coherent and incoherent detection," *IEEE Transactions on Terahertz Science and Technology*, vol. 1, no. 2, pp. 395–402, 2011.

[43] P. Bia, D. Caratelli, L. Mescia, and J. Gielis, "Electromagnetic characterization of supershaped lens antennas for high-frequency applications," in *Proceedings of the 43rd European Microwave Conference*, pp. 1679–1682, 2013.

[44] M. Planck, "Über das Gesetz der Energieverteilung im Normalspektrum," *Annalen der Physik*, vol. 4, pp. 553–558, 1901.

[45] V. Marian, B. Allard, C. Vollaire, and J. Verdier, "Strategy for microwave energy harvesting from ambient field or a feeding source," *IEEE Transactions on Power Electronics*, vol. 27, no. 11, pp. 4481–4491, 2012.

[46] A. Costanzo, A. Romani, D. Masotti, N. Arbizzani, and V. Rizzoli, "RF/baseband co-design of switching receivers for multiband microwave energy harvesting," *Sensors and Actuators A*, vol. 179, pp. 158–168, 2012.

[47] U. Olgun, C. Chen, and J. L. Volakis, "Investigation of rectenna array configurations for enhanced RF power harvesting," *IEEE Antennas and Wireless Propagation Letters*, vol. 10, pp. 262–265, 2011.

[48] H. Kazemi, K. Shinohara, G. Nagy et al., "First THz and IR characterization of nanometer-scaled antenna-coupled InGaAs/InP Schottky-diode detectors for room temperature infrared imaging," in *Infrared Technology and Applications XXXIII, 65421J*, vol. 6542 of *Proceedings of SPIE*, Orlando, Fla, USA, April 2007.

[49] C. Balocco, S. R. Kasjoo, L. Q. Zhang, Y. Alimi, and A. M. Song, "Low-frequency noise of unipolar nanorectifiers," *Applied Physics Letters*, vol. 99, no. 11, Article ID 113511, 2011.

[50] C. Balocco, S. R. Kasjoo, X. F. Lu et al., "Room-temperature operation of a unipolar nanodiode at terahertz frequencies," *Applied Physics Letters*, vol. 98, no. 22, Article ID 223501, 2011.

[51] C. Balocco, M. Halsall, N. Q. Vinh, and A. M. Song, "THz operation of asymmetric-nanochannel devices," *Journal of Physics Condensed Matter*, vol. 20, no. 38, Article ID 384203, 2008.

[52] G. Farhi, E. Saracco, J. Beerens, D. Morris, S. A. Charlebois, and J.-P. Raskin, "Electrical characteristics and simulations of self-switching-diodes in SOI technology," *Solid-State Electronics*, vol. 51, no. 9, pp. 1245–1249, 2007.

[53] L. A. Majewski, C. Balocco, R. King, S. Whitelegg, and A. M. Song, "Fast polymer nanorectifiers for inductively coupled RFID tags," *Materials Science and Engineering B*, vol. 147, no. 2-3, pp. 289–292, 2008.

[54] J. Kettle, R. M. Perks, and R. T. Hoyle, "Fabrication of highly transparent self-switching diodes using single layer indium tin oxide," *Electronics Letters*, vol. 45, no. 1, pp. 79–81, 2009.

[55] A. Hammar, S. Cherednichenko, S. Bevilacqua, V. Drakinskiy, and J. Stake, "Terahertz direct detection in $YBa_2Cu_3O_7$ microbolometers," *IEEE Transactions on Terahertz Science and Technology*, vol. 1, no. 2, pp. 390–394, 2011.

[56] B. S. Karasik, A. V. Sergeev, and D. E. Prober, "Nanobolometers for THz photon detection," *IEEE Transactions on Terahertz Science and Technology*, vol. 1, no. 1, pp. 97–111, 2011.

[57] S. Agarwal and E. Yablonovitch, "Using dimensionality to achieve a sharp tunneling FET (TFET) turn-on," in *Proceedings of the 69th Device Research Conference (DRC '11)*, pp. 199–200, Santa Barbara, Calif, USA, June 2011.

[58] S. Bhansali, S. Krishnan, E. Stefanakos, and D. Y. Goswami, "Tunnel junction based rectenna—a key to ultrahigh efficiency solar/thermal energy conversion," in *Proceedings of the International Conference on Physics of Emerging Functional Materials (PEFM '10)*, pp. 79–83, Mumbai, India, September 2010.

[59] D. Dragoman and M. Dragoman, "Geometrically induced rectification in two-dimensional ballistic nanodevices," *Journal of Physics D: Applied Physics*, vol. 46, no. 5, Article ID 055306, 2013.

[60] H. Choo, M.-K. Kim, M. Staffaroni et al., "Nanofocusing in a metal-insulator-metal gap plasmon waveguide with a three-dimensional linear taper," *Nature Photonics*, vol. 6, no. 12, pp. 838–844, 2012.

[61] M. Schnell, P. Alonso-González, L. Arzubiaga et al., "Nanofocusing of mid-infrared energy with tapered transmission lines," *Nature Photonics*, vol. 5, no. 5, pp. 283–287, 2011.

[62] Z. Zhu, S. Joshi, S. Grover, and G. Moddel, "Graphene geometric diodes for terahertz rectennas," *Journal of Physics D: Applied Physics*, vol. 46, no. 18, Article ID 185101, 2013.

[63] A. M. Song, A. Lorke, A. Kriele, J. P. Kotthaus, W. Wegscheider, and M. Bichler, "Nonlinear electron transport in an asymmetric microjunction: a ballistic rectifier," *Physical Review Letters*, vol. 80, no. 17, pp. 3831–3834, 1998.

[64] S. Krishnan, Y. Goswami, and E. Stefanakos, "Nanoscaale Rectenna for thermal energy conversion to electricity," *Technology & Innovation*, vol. 14, no. 2, pp. 103–113, 2012.

[65] M. A. Darrin, R. Osiander, J. Lehtonen, D. Farrar, D. Douglas, and T. Swanson, "Novel micro electro mechanical systems (MEMS) packaging for the skin of the satellite," in *Proceeding of the IEEE Aerospace Conference*, vol. 4, pp. 2486–2492, Big Sky, Mont, USA, March 2004.

[66] G. Moddel, "Chapter 1. Will rectenna solar cells be practical?" in *Rectenna Solar Cells*, G. Moddel and S. Grover, Eds., pp. 3–24, Springer, New York, NY, USA, 2013.

[67] Y. Mastai, Y. Diamant, S. T. Aruna, and A. Zaban, "TiO_2 nanocrystalline pigmented polyethylene foils for radiative cooling applications: synthesis and characterization," *Langmuir*, vol. 17, no. 22, pp. 7118–7123, 2001.

[68] B. E. Hardin, E. T. Hoke, P. B. Armstrong et al., "Increased light harvesting in dye-sensitized solar cells with energy relay dyes," *Nature Photonics*, vol. 3, no. 11, p. 667, 2009.

[69] A. Massaro, F. Spano, M. Missori et al., "Flexible nanocomposites with all-optical tactile sensing capability," *RSC Advances*, vol. 4, no. 6, pp. 2820–2825, 2014.

[70] S. Soumya, A. Mohamed, P. Paul, L. Mohan, and K. Ananthakumar, "Near IR reflectance characteristics of PMMA/ZnO nanocomposites for solar thermal control interface films," *Solar Energy Materials & Solar Cells*, vol. 125, pp. 102–112, 2014.

[71] M. Yu, Y. Long, B. Sun, and Z. Fan, "Recent advances in solar cells based on one-dimensional nanostructure arrays," *Nanoscale*, vol. 4, no. 9, pp. 2783–2796, 2012.

[72] W. F. van Dorp and C. W. Hagen, "A critical literature review of focused electron beam induced deposition," *Journal of Applied Physics*, vol. 104, no. 8, Article ID 081301, 2008.

[73] A. Weber-Bargioni, A. Schwartzberg, M. Schmidt et al., "Functional plasmonic antenna scanning probes fabricated by induced-deposition mask lithography," *Nanotechnology*, vol. 21, Article ID 065306, 2010.

[74] J. Orlo, M. Utlaut, and L. Swanson, *High Resolution Focused Ion Beams: FIB and Applications*, Kluwer Academic/Plenum Publishers, 2002.

[75] S. Y. Chou, P. R. Krauss, and P. J. Renstrom, "Nanoimprint lithography," *Journal of Vacuum Science and Technology B*, vol. 14, no. 6, pp. 4129–4133, 1996.

[76] K. Jain, "Flexible electronics and displays: high-resolution, roll-to-roll, projection lithography and photoablation processing technologies for high-throughput production," *Proceedings of the IEEE*, vol. 93, no. 8, pp. 1500–1510, 2005.

[77] M. D. Stewart and C. G. Willson, "Imprint materials for nanoscale devices," *MRS Bulletin*, vol. 30, no. 12, pp. 947–951, 2005.

[78] C. Y. Chang, S. Y. Yang, and J. L. Sheh, "A roller embossing process for rapid fabrication of microlens arrays on glass substrates," *Microsystem Technologies*, vol. 12, no. 8, pp. 754–759, 2006.

[79] S. Youn, M. Ogiwara, H. Goto, M. Takahashi, and R. Maeda, "Prototype development of a roller imprint system and its application to large area polymer replication for a microstructured optical device," *Journal of Materials Processing Technology*, vol. 202, no. 1–3, pp. 76–85, 2008.